DOI: 10.1002/chem.200802222

Oxidant-Free Dehydrogenation of Alcohols Heterogeneously Catalyzed by Cooperation of Silver Clusters and Acid–Base Sites on Alumina

Ken-ichi Shimizu,* Kenji Sugino, Kyoichi Sawabe, and Atsushi Satsuma[a]

Abstract: A γ-alumina-supported silver cluster catalyst—Ag/Al_2O_3—has been shown to act as an efficient heterogeneous catalyst for oxidant-free alcohol dehydrogenation to carbonyl compounds at 373 K. The catalyst shows higher activity than conventional heterogeneous catalysts based on platinum group metals (PGMs) and can be recycled. A systematic study on the influence of the particle size and oxidation state of silver species, combined with characterization by Ag K-edge XAFS (X-ray absorption fine structure) has established that silver clusters of sizes below 1 nm are responsible for the higher specific rate. The reaction mechanism has been investigated by kinetic studies (Hammett correlation, kinetic isotope effect) and by in situ FTIR (kinetic isotope effect for hydride elimination reaction from surface alkoxide species), and the following mechanism is proposed: 1) reaction between the alcohol and a basic OH group on the alumina to yield alkoxide on alumina and an adsorbed water molecule, 2) C–H activation of the alkoxide species by the silver cluster to form a silver hydride species and a carbonyl compound, and 3) H_2 desorption promoted by an acid site in the alumina. The proposed mechanism provides fundamental reasons for the higher activities of silver clusters on acid–base bifunctional support (Al_2O_3) than on basic (MgO and CeO_2) and acidic to neutral (SiO_2) ones. This example demonstrates that catalysts analogous to those based on of platinum group metals can be designed with use of a less expensive d^{10} element—silver—through optimization of metal particle size and the acid–base natures of inorganic supports.

Keywords: alcohols · C–H activation · green chemistry · heterogeneous catalysis · silver

Introduction

Materials with clusters have interesting chemical properties unusual for bulk solids. Size- and support-specific catalysis by supported gold clusters is a well known example.[1–8] Various supported gold catalysts have been reported to show catalytic activities similar to or higher than those of platinum group metals (PGMs) for oxidation of alcohols to carbonyl compounds,[4–8] as well as for CO oxidation.[1–3] However, fundamental aspects of the size- and support-specific catalysis of these reactions still remained controversial. One might expect that silver, as a less expensive group IB metal, should be usable for the design of PGM-free catalysts through optimization of metal particle size and support. Silver clusters appear to be very popular in the research field of nanoparticle synthesis,[9–13] and several review articles have been published.[9,10] The number of investigations that have focused on specific catalysis by silver clusters or nanoparticles, however, is surprisingly small in comparison with research into gold nanoparticle catalysis.[14–24]

We have been paying attention to cluster-specific catalysis by supported silver catalysts for environmental applications and have reported a series of studies on size- and support-specific catalysis by silver clusters for the selective catalytic reduction of NOx with hydrocarbons for the removal of NOx emissions from diesel engine exhausts.[20–22] It has been shown that, of various silver catalysts, silver clusters on alumina constitute the best catalyst, with activity much higher than that of Pt/Al_2O_3 catalyst. Fundamental studies showed that both the silver clusters and the acid–base sites on the support surface are responsible for the high activity of silver clusters on alumina.[20–22] For this study we attempted an extension of the acid–base-assisted silver cluster catalysis to selective oxidation.

C–H activation catalysis, including oxidation of alcohols to carbonyl compounds, is one of the most important topics

[a] Dr. K.-i. Shimizu, K. Sugino, Dr. K. Sawabe, Prof. Dr. A. Satsuma
Department of Molecular Design and Engineering
Graduate School of Engineering, Nagoya University
Nagoya 464-8603 (Japan)
Fax: (+81) 52-789-3193
E-mail: kshimizu@apchem.nagoya-u.ac.jp

in the fields of catalysis and organic chemistry. To achieve environmental and economical acceptability, much effort has been devoted to the development of transition-metal-catalyzed oxidation of alcohols with environmentally friendly oxidants (such as oxygen, hydrogen peroxide, or alkenes) that avoid the use of large excesses of toxic and expensive stoichiometric metal oxidants.[3–7,25–30] From the viewpoint of atom efficiency and safety of the reaction, an oxidant-free catalytic dehydrogenation of alcohols to carbonyl compounds and molecular hydrogen would be ideal. Several recent reports show oxidant-free alcohol dehydrogenation with PGM catalysts (ruthenium[31–35] and iridium[36] complexes and heterogeneous ruthenium catalysts[37–39]). However, they suffer variously from the need for acid or base additives, from difficulties in catalyst synthesis, manipulation, or reusability, from high cost, or from low activity for the primary alcohol dehydrogenation. Very recently, Mitsudome et al. have developed Ag- or Cu-based heterogeneous catalysts for the oxidant-free dehydrogenation of alcohols.[23,40] In particular, Ag/HT (hydrotalcite-supported silver nanoparticles) are attractive as the most active catalyst for this reaction,[23] although the reaction mechanism and the origins of the size- and support-specific catalysis are not well established. Understanding of how silver-based catalysts operate is imperative for the rational development of improved PGM-free alcohol dehydrogenation catalysts.

In the research area of organometallic catalysis, attention has been focused on the cooperation of acid or basic ligands in organic reactions catalyzed by transition metal complexes.[28,35,36,41–44] One of the successful examples is Noyori's ruthenium catalyst for the hydrogenation of polar bonds, in which cooperation between an acidic hydrogen on an amido ligand and ruthenium hydride plays an important role.[41] For the catalytic dehydrogenative oxidation of alcohols, Fujita et al. developed an iridium complex containing a 2-hydroxypyridine ligand. The hydride ion on iridium, formed by C–H cleavage of an iridium alkoxide intermediate, can be effectively removed through its reaction with the protic hydrogen on the ligand, which facilitates the release of dihydrogen.[36] A ruthenium catalyst developed by Milstein's group possesses a cooperative basic site in a β position to the metal, which facilitates binding of the alcohol substrate to give an alkoxide intermediate.[35] Knowing that metal oxides, such as γ-alumina, have acid–base sites on their surfaces, one might expect that the cooperative effect of the organic ligand might be replaceable by that of an inorganic support material.

Here we demonstrate a well characterized γ-alumina-supported silver cluster as an effective heterogeneous catalyst for the oxidant-free catalytic dehydrogenation of alcohols to carbonyl compounds. We report detailed mechanistic and structural studies that address the influence of the size and charge state of silver and the nature of the support to establish a detailed reaction mechanism that should be useful for the design of practical heterogeneous catalysts without use of organic ligands and PGM elements. We adopted two complementary ways of studying the mechanism of a catalytic process: one involves kinetic measurements for the overall reaction, and the other direct spectroscopic observation of the C–H activation step in a catalytic cycle. Combination of these approaches should give full understanding of the catalytic process.

Results and Discussion

Characterization of Al_2O_3-supported Ag clusters: The X-ray diffraction (XRD) pattern of Ag/Al_2O_3-x ($x=1$–10 wt %; see Experimental Section for terminology) was essentially the same as that of the γ-Al_2O_3 support, and no lines due to Ag metal or Ag_2O were observed, indicating no formation of large Ag metal or Ag_2O particles during the catalyst preparation. In this study, Ag/Al_2O_3 catalysts were reduced with H_2 at 573 K before each catalytic reaction. To investigate the structure of Ag species after the H_2 reduction, in situ Ag K-edge XAFS measurement of Ag/Al_2O_3 and Ag reference compounds was carried at 573 K. Figure 1A shows Ag K-edge X-ray absorption near-edge structures (XANES) spectra, which are known to be sensitive to the oxidation states of X-ray absorbing atoms. The XANES feature of Ag/Al_2O_3-x ($x=1$–10 wt %) after the H_2 reduction is clearly different from that of Ag_2SO_4 but rather similar to that of Ag powder, indicating that silver species in these samples are in a reduced state. On the other hand, the XANES features of Ag/Al_2O_3-5 before the reduction and Ag/Al_2O_3-0.5 after the reduction differ from that of Ag powder but resemble that of Ag_2SO_4 as a reference compound for ionic Ag^+ species surrounded by oxygen atoms. This suggests that Ag^+ is the dominant silver species in the H_2-reduced Ag/Al_2O_3-0.5 and unreduced Ag/Al_2O_3-5 samples.

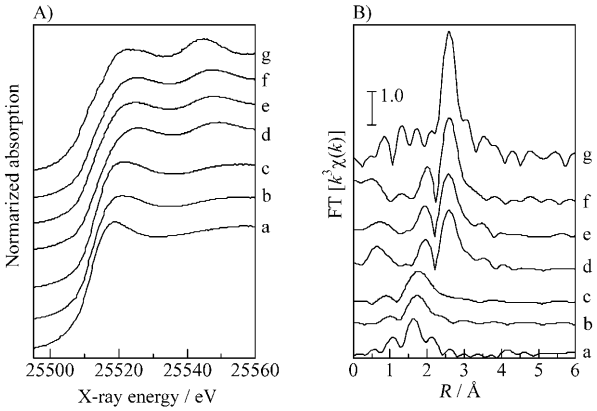

Figure 1. Ag K-edge A) XANES spectra and B) EXAFS Fourier transforms recorded in situ after flowing of various gas mixtures for 0.5 h at 573 K: a) Ag_2SO_4 in He, b) Ag/Al_2O_3-5 in O_2 (10 %), c) Ag/Al_2O_3-0.5 in H_2 (1 %), d) Ag/Al_2O_3-1 in H_2 (1 %), e) Ag/Al_2O_3-5 in H_2 (1 %), f) Ag/Al_2O_3-10 in H_2 (1 %), and g) Ag powder in He.

Figure 1B shows the Fourier transform (FT) of the k^3-weighted Ag K-edge extended X-ray absorption fine structure (EXAFS) of Ag/Al_2O_3 and Ag powder. The structural parameters derived from curve-fitting analysis are listed in

Table 1. The EXAFS of the fresh Ag/Al_2O_3-5 (spectrum a) showed large Ag–O contribution, and the Ag–Ag coordination number was negligibly small (Table 1). When the flowing gas was switched from O_2 (10%) to H_2 (1%), the spectral feature changed. After H_2 reduction at 573 K for 30 min (spectrum e), the Ag–Ag shell with coordination number of 5.9 and bond length of 2.85 Å was observed. The Ag–O coordination number decreased from 1.2 to 0.5 and the Ag–Ag coordination number increased from 0.3 to 5.9 after the reduction. For the Ag/Al_2O_3 samples with Ag loadings of 1–10 wt%, the Ag–Ag contribution with the bond length of 2.84–2.85 Å was also observed. This distance is shorter than that in bulk Ag and is close to the Ag–Ag distance reported for silver clusters in Ag-exchanged zeolite X formed by H_2 reduction at 573 K.[13] The Ag–Ag coordination numbers (5.0–7.8) were lower than that of bulk Ag(12). These results indicate that the H_2 reduction treatment results in the reduction and aggregation of Ag^+ ions to metallic silver clusters. In the EXAFS for the lowest loading sample—Ag/Al_2O_3-0.5—the Ag–Ag contribution was negligibly small even after 30 min of the reduction treatment (spectrum c), indicating that reductive agglomeration of Ag^+ to silver cluster does not occur in this sample. In summary, the EXAFS and XANES results show that small silver clusters are the predominant silver species on the Ag/Al_2O_3-x (x = 1–10 wt%), whereas on Ag/Al_2O_3-0.5 most of the silver species are highly dispersed as Ag^+ ions. The Ag–O EXAFS contributions with coordination numbers of 0.5–0.6 in Ag/Al_2O_3-x (x = 1–10 wt%) samples suggest that silver clusters are not fully reduced and may exist as cationic clusters interacting with oxygen atoms at the metal surface or the metal–support interface.

Table 1. Curve-fitting analysis of Ag K-edge in situ EXAFS at 573 K in H_2 (1%) for Ag/Al_2O_3.

Catalyst[a]	Shell	CN[b]	R [Å][c]	(σ^2)[d] [Å^2]	R_f [%][e]
0.5	O	2.3	2.23	0.100	8.1
	Ag	0.2	2.76	0.003	
1	O	0.5	2.24	0.015	2.3
	Ag	5.0	2.85	0.068	
3	O	0.5	2.26	0.015	1.9
	Ag	5.4	2.84	0.079	
5	O	0.5	2.25	0.010	1.8
	Ag	5.9	2.85	0.076	
5 (O_2)[f]	O	1.2	2.17	0.070	4.7
	Ag	0.3	2.72	0.028	
10	O	0.6	2.26	0.005	2.9
	Ag	7.8	2.85	0.081	

[a] Ag loading (wt%) on Ag/Al_2O_3. [b] Coordination numbers. [c] Bond length. [d] Debye–Waller factor. [e] Residual factor. [f] EXAFS data for the Ag/Al_2O_3-5 sample before H_2 reduction recorded under O_2 (10%) at 573 K.

Catalytic properties: With the Ag/Al_2O_3-5 as a standard catalyst, we examined its catalytic activity for the oxidant-free oxidation of alcohols. When 4-methylbenzyl alcohol was treated in the presence of Ag/Al_2O_3-5 (2.0 mol% of Ag) at 373 K in toluene for 24 h, 4-methylbenzaldehyde was produced in 93% yield and with 93% selectivity at a level of alcohol conversion of 99% (Table 2, entry 1). After 12 h reaction time, the yields of gas-phase H_2 (75%) and 4-methylbenzaldehyde (76%) were nearly identical to the level of conversion of the alcohol (77%), indicating that H_2 was generated quantitatively during the dehydrogenation. Because H_2 escapes from the reaction mixture into the gas phase, the overall endothermic dehydrogenation reaction is driven to the product side.

The dehydrogenation of 4-methylbenzyl alcohol was completely stopped by the removal of Ag/Al_2O_3-5 from the reaction mixture: the catalyst was filtered off after the reaction mixture had been stirred for 2 h (yield 37%), and the reaction then did not proceed further when the filtrate was heated at 373 K for 22 h. This result rules out any possible contribution of homogeneous catalysis by leached silver species.

We also studied reuse of the Ag/Al_2O_3-5 catalyst, with the dehydrogenation of 4-methylbenzyl alcohol as test reaction. The catalyst can be easily separated from the reaction mixture by simple filtration. Although the filtered catalyst showed a decrease in activity (64% yield), its activity was once more restored to that observed for the first run (entry 1) after the filtered catalyst had been calcined in air at 873 K for 10 min, followed by the reduction with H_2 at 573 K for 5 min (entries 2, 3 and 4).

Table 2. Dehydrogenation of various alcohols.[a]

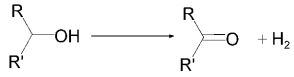

Entry	Substrate	Product	Conv. [%]	Yield [%]
1	4-methylbenzyl alcohol	4-methylbenzaldehyde	99	93
2[b]			99	90
3[c]			99	94
4[d]			99	91
5	benzyl alcohol	benzaldehyde	100	82
6	4-methoxybenzyl alcohol	4-methoxybenzaldehyde	100	86
7[e]	4-chlorobenzyl alcohol	4-chlorobenzaldehyde	79	70
8	1-phenylethanol	acetophenone	99	93
9[e]	octan-2-ol	octan-2-one	53	50
10[f]	propan-2-ol	acetone	82	80
11[e]	cyclohexanol	cyclohexanone	72	70
12[e]	cyclodecanol	cyclodecanone	100	94
13[e]	octan-1-ol	1-octanone	27	16

[a] Substrate (1.0 mmol), toluene (3 mL), Ag/Al_2O_3-5 catalyst (2.0 mol%), T = 373 K, t = 24 h. Levels of conversion of the alcohols and yields of carbonyl compounds were determined by GC. [b] Reuse 1. [c] Reuse 2. [d] Reuse 3. [e] t = 48 h. [f] T = 353 K.

The total turnover number (TON) based on total Ag content was 184, which is comparable with those reported for oxidant-free secondary alcohol dehydrogenation with some homogeneous Ru catalysts (TONs: 160 to 186).[31–35] The commercially available PGM-based heterogeneous catalysts Ru/C, Ru/Al_2O_3, Pd/C, and Pd/Al_2O_3 (Ru or Pd = 5 wt%) were tested for the oxidant-free dehydrogenation of 4-methylbenzyl alcohol under conditions similar to those in Table 2 (entry 1). After treatment at 373 K in toluene for 60 h, 4-methylbenzaldehyde yields with Ru/C, Ru/Al_2O_3, Pd/C, and Pd/Al_2O_3 were 14, 81, 20, and 56%, respectively, which were less than the yield obtained with Ag/Al_2O_3-5 (93% after 24 h). This result clearly demonstrates higher catalytic efficiency of Ag/Al_2O_3-5 for this reaction.

The scope of alcohol dehydrogenation by Ag/Al_2O_3-5 was studied (Table 2). Oxidation of benzyl alcohol proceeded with moderate selectivity (82%); small amounts of benzyl benzoate (1%) and dibenzyl ether (2%) were obtained as side products. The oxidation of *p*-substituted benzyl alcohols proceeded with good yields. It should be noted that most of the previously reported homogeneous transition metal complexes are unable to catalyze the oxidant-free dehydration of primary alcohols.[31–36] Secondary alcohols, including the less reactive aliphatic alcohols (cyclohexanol, cyclodecanol, propan-2-ol, and octan-2-ol), were also tolerated with good to moderate yields. Treatment of octan-1-ol produced octanal only in 16% yield after 48 h, but the production of octyl octanoate was negligible.

Structure–activity relationships: The reaction rates for the dehydrogenation of benzyl alcohol were measured under conditions where levels of conversion were below 30% for a series of Ag/Al_2O_3 catalysts with different Ag loadings. Figure 2A plots the benzaldehyde formation rate per gram of Ag/Al_2O_3 as a function of silver loading. The catalyst with lowest loading (0.5 wt%) is nearly inactive. The rate increased with the silver loading up to 5 wt% and then decreased with further increases in the loading.

To investigate the relationship between structure and catalytic activity, we also examined the effect of silver loading on the particle size of metallic silver species in Ag/Al_2O_3. By using the coordination number of Ag–Ag contribution in EXAFS (Table 1), the average metallic silver cluster size was determined by the model of Jentys.[45] The average silver powder particle size (a plot for Ag loading of 100% in Figure 2B) was estimated from the XRD line broadening of the Ag(111) reflection at $2\theta = 38.1°$ due to Ag metal by use of the Scherrer equation. As shown in Figure 2B, the average silver cluster size increased with silver loading. By using the mean diameter of silver clusters and the atomic diameter of silver (0.289 nm) and by assuming that the supported silver clusters can be modeled as a fcc crystal lattice, the number of surface silver atoms for each catalyst was statistically determined according to the methods of Mori et al.[26] and Abad et al.[6] This value was then used to estimate turnover frequency (TOF) per surface Ag site as shown in Figure 2C. Above 1 wt%, at which silver species

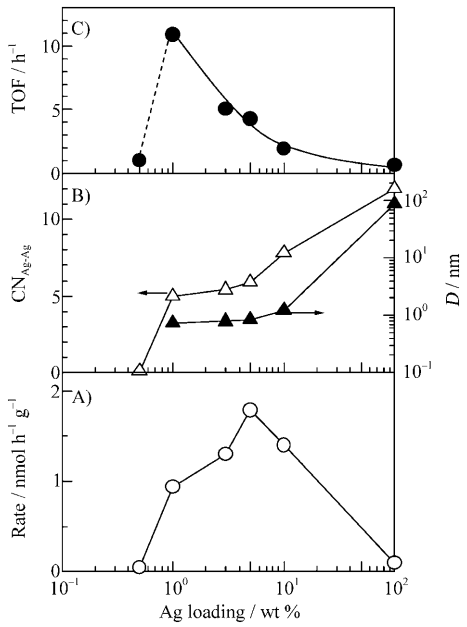

Figure 2. Effect of Ag loading of Ag/Al_2O_3 on ○) the initial rate, and ●) TOF based on the number of surface Ag atoms for dehydrogenation of benzyl alcohol at 373 K. △) CN for Ag–Ag shell of EXAFS (from Table 1), and ▲) average particle size of Ag from the EXAFS analysis.

are present mainly as metal clusters, TOF per surface Ag atoms decreases with increase in Ag loading. The TOF per surface Ag sites versus average particle size is shown in Figure 3. Clearly, the intrinsic activity per external silver

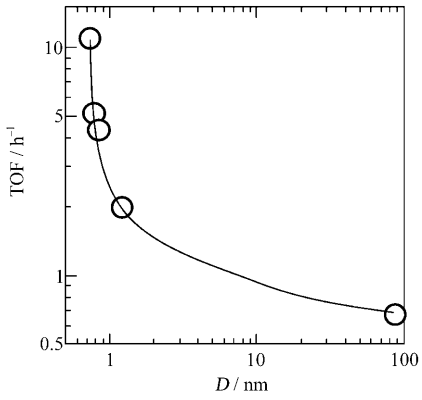

Figure 3. ○) TOF based on the number of surface Ag atoms for dehydrogenation of benzyl alcohol at 373 K as a function of average particle size of Ag in Ag/Al_2O_3-x (x = 1–100 wr%) catalysts (from Figure 1).

atom decreases with the particle size. From these quantitative studies, the following conclusions relating to the structure–activity relationship can be drawn. The silver cluster acts as a more efficient catalytic site for alcohol dehydrogenation than monomeric Ag^+ ion and bulk Ag particle, and the silver clusters with smaller particle sizes give higher intrinsic activity.

To examine the role of the support in silver-catalyzed dehydrogenation of alcohols, we prepared a series of supported silver catalysts with the same silver content (5 wt%) and of similar particle size (0.8–3.0 nm), but with a variety of supports. EXAFS and XANES analysis of these catalysts showed that silver clusters with mean particle size of 0.8 to 2.9 nm make up the main silver species on these catalysts (results not shown). The catalytic activities and selectivities in the dehydrogenation of 4-methylbenzyl alcohol with various silver catalysts were measured, and the aldehyde yields were plotted as a function of the electronegativities of the metal species in the support materials, which have been used as a parameter for the acidity of metal oxides (Figure 4). There is a volcano-type relationship between the

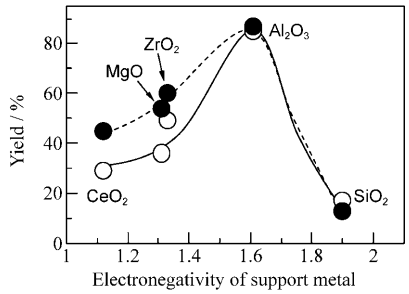

Figure 4. Yield of *p*-methylbenzaldehyde (from Table 2) as a function of the electronegativity of support cation under N_2 (○) or O_2 (●).

catalytic activity and the electronegativity. The silver clusters supported on alumina, which is known to have both acidic and basic surface sites,[46,47] had the highest catalytic activity. The supports with low electronegativity (strong basic character) gave lower yields. The silver clusters on SiO_2, which can be regarded as an acidic or neutral oxide,[48] had lowest activity. These results suggest that both acidic and basic surface sites are necessary for the efficient catalytic dehydrogenation of alcohols.

Reaction mechanism: The adsorption complexes formed from the adsorption of propan-2-ol (0.5 mmol per g catalyst) on various reference oxides and Ag/Al_2O_3-5 at 313 K were studied in situ by FTIR spectroscopy (Figure 5). The result for Ag/Al_2O_3-5 (spectrum d) shows the predominance of very strong bands at 2970 cm^{-1}(methyl asymmetric C–H stretching), 2940 cm^{-1} (methyl asymmetric C–H stretching), 2874 cm^{-1} (coupling of α-C–H stretching and methyl symmetric C–H stretching), 1465 cm^{-1} (methyl asymmetric deformation), 1376 cm^{-1} (methyl symmetric deformation), 1328 cm^{-1} (α-C–H deformation), 1166 and 1130 cm^{-1} (C–O/C–C coupled stretchings) typical of 2-propoxide groups.[49,50] A very weak peak at 2640 cm^{-1} may correspond to a combination of the C–O/C–C coupled stretchings (1166 cm^{-1}) and the methyl deformation (1465 cm^{-1}) of the 2-propoxide, as previously reported for FTIR study of methanol adsorption on alumina.[51] A band at 1280 cm^{-1} due to OH deformation of the propan-2-ol molecule is hardly observable, which indicates the absence of non-dissociatively adsorbed propan-2-ol on the catalyst.

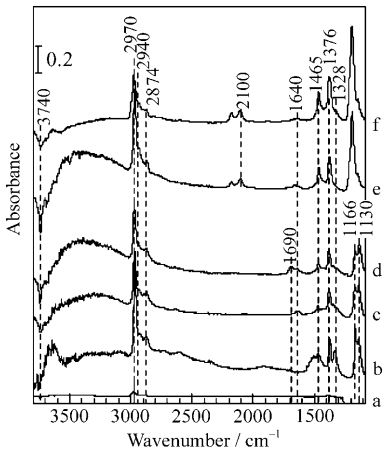

Figure 5. IR spectra after exposure to propan-2-ol (0.5 mmol per g catalyst), followed by purging with He for 60 s at 313 K: a) SiO_2, b) MgO, c) Al_2O_3, and d) Ag/Al_2O_3-5. Spectra e and f are results for $[D_2]$propan-2-ol adsorption at 313 K on Ag/Al_2O_3-5 and Al_2O_3, respectively.

In the FTIR spectrum of the adsorbed species formed by the reaction between Ag/Al_2O_3-5 and $[D_2]$propan-2-ol (α-deuteriated propan-2-ol), bands at 2970 cm^{-1}(methyl asymmetric C–H stretching), 2940 cm^{-1} (methyl asymmetric C–H stretching), 2870 cm^{-1} (methyl symmetric C–H stretching), 2100 cm^{-1} (α-C–D stretching), 1465 cm^{-1} (methyl asymmetric deformation), 1376 cm^{-1} (methyl symmetric deformation), 1328 cm^{-1} (α-C–H deformation), 1190 cm^{-1} (C–O/C–C coupled stretchings) were assigned to α-deuteriated 2-propoxide groups. A weak band at 2140 cm^{-1} may be assigned to a different type of 2-propoxide species. It is noteworthy that in both propan-2-ol and $[D_2]$propan-2-ol adsorption experiments the IR spectra for Al_2O_3 (spectra c, f) were basically the same spectra as seen for Ag/Al_2O_3-5 (spectra d, e), suggesting that 2-propoxide is adsorbed not on the silver site, but on the surface of the Al_2O_3.

Immediately after introduction of propan-2-ol onto the catalyst ($t = 60$ s), an intense negative peak at about 3740 cm^{-1} was observable in the OH stretching region; this has been attributed to the surface OH-μ_2-Al group.[47] Broad overlapping bands centered around 3300 cm^{-1} in the OH stretching region and a weak feature at 1640 cm^{-1} were also observed. These are characteristic of the OH stretching vibration and the HOH bending vibration of adsorbed water.[52] It is established that hydrogen bonding causes the downward shift and broadening of the OH stretching bands of the surface hydroxy groups.[48] The broad feature due to OH stretching vibration suggests that the water molecules are strongly hydrogen bonded. A similar IR spectrum with a negative peak at about 3750 cm^{-1} and bands due to adsorbed water was observed for η-alumina after HCl adsorption, which was interpreted as arising from the reaction between Al–OH with HCl to yield AlCl and H_2O.[53] This indicates that the OH-μ_2-Al group acts as a Brønsted base, as has also been supported by a recent quantum chemical

study.[54] From these observations the following surface reaction [Eq. (1)] is established: the reaction between propan-2-ol and a OH-μ_2-Al group (Brønsted base site) results in the formation of 2-propoxide coordinated to the unsaturated Al site (Lewis acid site) and a hydrogen-bonded water molecule on the alumina surface.

$$(CH_3)_2CHOH+Al-OH \rightarrow (CH_3)_2CH-O-Al+H_2O \quad (1)$$

To investigate the reaction behavior of 2-propoxide species, the reaction between propan-2-ol and Ag/Al_2O_3-5 at 373 K was studied by in situ FTIR (Figure 6A). After rapid formation of the 2-propoxide species ($t=60$ s), the intensities of the bands due to the 2-propoxide species gradually decreased and a new band at 1690 cm^{-1}, due to C=O stretching of acetone adsorbed on alumina,[55] appeared and its intensity increased with time. This suggests that 2-propoxide undergoes C–H cleavage, resulting in the formation of acetone. Note that 2-propoxide species on silver-free alumina did not convert to acetone in a temperature range of 313–373 K. This indicates that the silver clusters are necessary in the C–H activation step. We tentatively assume that the acetone formation [Eq. (3)] proceeds via silver hydride and carbocation intermediates [Eq. (2)], which was confirmed by liquid-phase kinetic studies. It is important to note that the propan-2-ol molecule introduced onto the catalyst surface was nearly completely converted into the 2-propoxide within 60 s, whereas 2-propoxide conversion to acetone occurred with much lower reaction rate than 2-propoxide formation. This result indicates that step (1) is faster than steps (2) and (3).

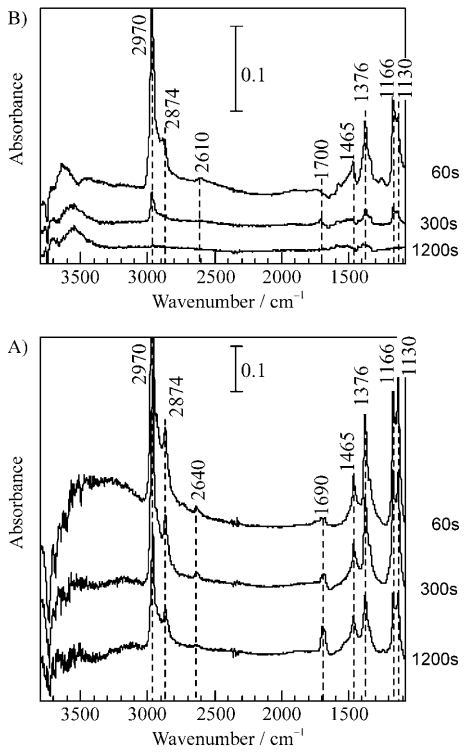

Figure 6. IR spectra taken at 373 K after exposure of A) Ag/Al_2O_3-5 or B) Ag/MgO-5 to propan-2-ol (0.5 mmol per g catalyst), followed by purging with He.

$$R_2CH-O-Al+Ag_n \rightarrow (CH_3)_2C^{\delta+}-O-Al+Ag_n-H^{\delta-} \quad (2)$$

$$(CH_3)_2C^{\delta+}-O-Al+H_2O \rightarrow (CH_3)_2C=O+H_2O\cdots Al \quad (3)$$

The intensities of the negative band at 3740 cm^{-1} and the band due to hydrogen-bonded water (3300 cm^{-1}) decreased with increasing reaction time, indicating the consumption of the hydrogen-bonded water to reproduce the OH-μ_2-Al group on the alumina surface. This can reasonably be interpreted as follows: the adsorbed water molecule reacts with the neighboring hydride ion to form dihydrogen, which results in a regeneration of a basic OH group of alumina [Eq. (4)].

$$Ag_n-H^{\delta-}+H_2O\cdots Al \rightarrow H_2+Al-OH+Ag_n \quad (4)$$

Kinetic analysis of the conversion of the 2-propoxide groups can be studied by the time-resolved IR method, and the result at 313 K is shown in Figure 7 as an example. The relative amounts of $(CH_3)_2CHO^-$ and $(CH_3)_2CDO^-$ groups were estimated from the changes in the areas of the IR bands in the 1080–1210 cm^{-1} or 1100–1250 cm^{-1} ranges, respectively, because these bands had the least overlap with other bands and, therefore, were the most suitable for the quantitative analysis. The first-order plots of 2-propoxide during its conversion into acetone gave fairly good straight lines. The first-order rate constants of 2-propoxide consumption at 313 K were estimated to be $3.2\times10^{-4}\pm7.4\times10^{-6}$ s^{-1} and $1.4\times10^{-4}\pm5.1\times10^{-6}$ s^{-1} for $(CH_3)_2CHO^-$ and $(CH_3)_2CDO^-$ groups, respectively. Figure 8 shows the rate constants for 2-propoxide consumption at a range of temperatures (313–373 K). Arrhenius plots for 2-propoxide consumption gave good straight lines, and the apparent activation energies determined from the slope were 27.3 ± 2.3 and 33.8 ± 1.3 kJ mol^{-1} for $(CH_3)_2CHO^-$ and $(CH_3)_2CDO^-$, respectively. The difference in these activation energies ($E_H-E_D=6.3\pm3.6$ kJ mol^{-1}) is consistent within experimental error with the zero-point energy difference (4.6 kJ mol^{-1}) between α-C–H (2874 cm^{-1}) and α-C–D (2100 cm^{-1}) estimated from the stretching vibration energies of 2-propoxide species. This indicates that the rate-determining step of 2-propoxide conversion to acetone is the cleavage of the C–H bond on the α-carbon atom.

Next, we studied kinetic experiments for the overall liquid-phase reaction with Ag/Al_2O_3-5 catalyst. Firstly, the dependence of the initial reaction rate on the initial benzyl alcohol concentration (0.09 to 0.32 M) showed a nonlinear dependence (Figure 9A). Good linear correlation is observed in a Lineweaver–Burk plot (Figure 9B), indicating that the reaction follows Michaelis–Menten-type kinetics: first-order dependence on alcohol at the low concentration and zero-order dependence on alcohol at higher concentrations.

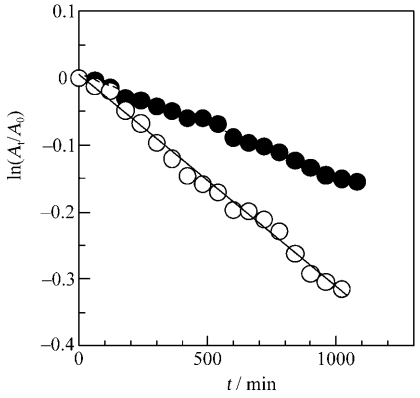

Figure 7. First-order plots for the decomposition of the surface 2-propoxide species on Ag/Al_2O_3-5 at 313 K. Rate constants estimated from the changes in the area of IR band in the 1080–1210 cm^{-1} range for $(CH_3)_2CHOH$ (○) and the 1100–1250 cm^{-1} range for $(CH_3)_2CDOH$ (●) were $3.2\times10^{-4}\pm7.4\ s^{-1}$ and $1.4\times10^{-4}\pm5.1\ s^{-1}$, respectively.

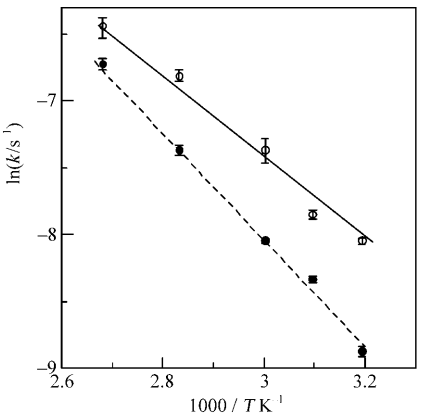

Figure 8. Arrhenius plots for the decomposition of surface 2-propoxide species on Ag/Al_2O_3-5. Apparent activation energies determined from the plots are 27.5 ± 2.3 and $33.8\pm1.3\ kJ\,mol^{-1}$ for $(CH_3)_2CHOH$ and $(CH_3)_2CDOH$, respectively.

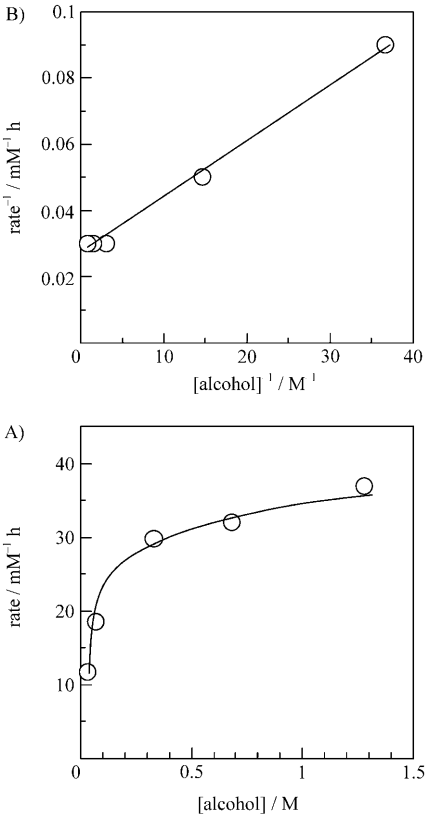

Figure 9. A) Rate dependence on the benzyl alcohol concentration, and B) Lineweaver–Burk plot. Conditions: benzyl alcohol (0.03–1.28 M), Ag/Al_2O_3-5 (2.0 mol%), toluene (3 mL), 373 K.

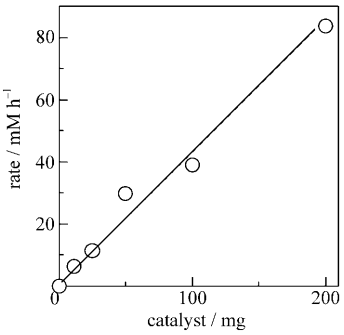

Figure 10. Effect of the amount of Ag/Al_2O_3-5 catalyst on the reaction rate for benzyl alcohol dehydrogenation. Conditions: Ag/Al_2O_3-5 (0.5–9.3 mol%), benzyl alcohol (1.0 mmol), toluene (3 mL), 373 K.

The dependence of the initial reaction rate on the amount of the catalyst is shown in Figure 10. The result shows that the rate has a linear relationship with the silver content in the system, indicating a first-order dependence of the rate on the silver concentration in the reaction system. These results suggest that both catalyst and alcohol are involved in a rate-limiting step and therefore rule out the decomposition of silver hydride to regenerate the silver site as rate-determining. Because the observed saturation kinetics in [alcohol] point toward a pre-equilibrium between catalyst and substrate, it is unlikely that alcohol binding is rate-determining.

Kinetic isotope effects in the liquid-phase propan-2-ol dehydrogenation under N_2 at 353 K were studied with $(CH_3)_2CHOH$ or $(CH_3)_2CDOH$ as reactants and Ag/Al_2O_3-5 as catalyst (Figure 11). In the initial reaction period, the concentration of acetone increased linearly with time. From the slope of the lines, the kinetic isotope effect (k_H/k_D) at 353 K was estimated to be 2.6. Ando et al. reported a k_H/k_D value of 1.57 for the liquid-phase dehydrogenation of $(CH_3)_2CHOH$ and $(CH_3)_2CDOH$ to yield acetone and molecular hydrogen under reflux conditions (at 355.6 K) with a carbon-supported ruthenium catalyst, and they concluded that the cleavage of the α-C–H bond is facile and that the highest activation energy is required for the formation of molecular hydrogen.[37] The primary kinetic isotope effect of 2.6 observed in our case indicates that the cleavage of the α-C–H bond is the rate-determining step in the overall reaction in the presence of Ag/Al_2O_3-5. The validity of the

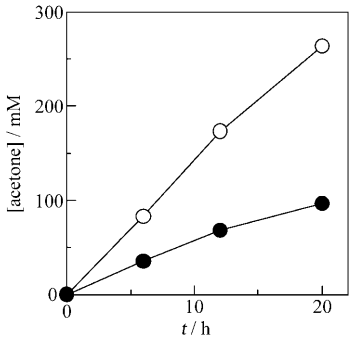

Figure 11. Isotopic effects in the dehydrogenation of $(CH_3)_2CHOH$ (○) and $(CH_3)_2CDOH$ (●) with Ag/Al_2O_3-5 as catalyst. Reaction conditions: alcohol (1.0 mmol), Ag/Al_2O_3-5 (2.0 mol%), toluene (3 mL), 353 K.

mechanism was also confirmed by a comparison of the reaction rate of a possible intermediate—2-propoxide—and the overall reaction rate as follows. The rate of the liquid-phase propan-2-ol dehydrogenation at 353 K ($0.83\,mmol\,g^{-1}\,h^{-1}$) was the same order of magnitude as the rate (ca. $1.98\,mmol\,g^{-1}\,h^{-1}$) estimated from the rate constant for the transient reaction of the 2-propoxide conversion to acetone at 353 K (Figure 8) and the initial surface coverage of the 2-propoxide.

Figure 12 shows the relationship between $\log(k_X/k_H)$ and the Brown–Okamoto (σ^+) or Hammett (σ) parameters for the competitive dehydrogenation of benzyl alcohol and *p*-substituted benzyl alcohols. Dehydrogenation of a series of different benzylic alcohols was catalyzed by Ag/Al_2O_3-5, and the order of reactivity found for substituted benzyl alcohols was *p*-CH_3O > *p*-CH_3 > *p*-H > *p*-Cl. There is fairly good linearity between $\log(k_X/k_H)$ and the σ^+ parameters, giving a negative slope ($\rho = -1.78$, $r^2 = 0.97$). The correlation with the σ^+ parameters had better fits than that with the σ parameters. These observations indicate that a transition state in the rate-determining step of the alcohol dehydration involves a positive charge at the α-carbon atom adjacent to the phenyl ring, which is stabilized by electron-donating substituents. In combination with the results of in situ IR and kinetic isotope effects, it was concluded that the rate-determining step in the overall reaction is the C–H activation of alkoxide species by silver clusters to form silver hydride species and carbonyl compound.

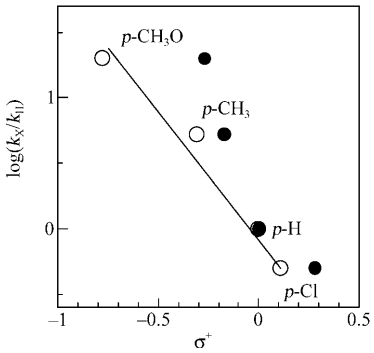

Figure 12. Hammett plots for competitive dehydrogenation of benzyl alcohol and *p*-substituted benzyl alcohols with Ag/Al_2O_3-5. $\log(k_X/k_H)$ versus σ^+ (○) and $\log(k_X/k_H)$ versus σ (●). Reaction conditions: benzyl alcohol (1.0 mmol), *p*-substituted benzyl alcohol (1.0 mmol), Ag/Al_2O_3-5 (2.0 mol%), toluene (3 mL). Slope (ρ^+) = – 1.78 ($r^2 = 0.97$).

A reaction mechanism based on the mechanistic and kinetic experiments for the dehydrogenation of alcohols by Ag/Al_2O_3-5 is presented in Scheme 1 in the case of propan-2-ol dehydrogenation as an example. The first step of the reaction is proton abstraction from the alcohol by a basic alumina OH-μ_2-Al group to yield an alkoxide group on an Al_{CUS} site (Lewis acid site) and a hydrogen-bonded water molecule on an acid site on the alumina surface. Alkoxide species at the interface between a silver cluster and alumina undergo hydride abstraction to yield hydride species on the silver cluster and acetone via a transition state with a positive charge at the α-carbon atom. The C–H cleavage step is rate-determining, as evidenced by the observation of the primary isotopic effects on 2-propoxide conversion to acetone (Figure 8) and overall propan-2-ol dehydrogenation (Figure 11). Next, a hydride ion on the silver cluster reacts with a water molecule adsorbed on a neighboring Lewis acid site to yield dihydrogen, accompanied by regeneration of a basic alumina OH group. It is reasonable to assume that Brønsted acidities of hydrogen atoms of adsorbed water are increased under the influence of alumina Lewis acid sites. This acid–base mechanism should facilitate the release of dihydrogen. The resulting hydride-free silver cluster and a basic alumina OH-μ_2-Al group are available in the next catalytic cycle.

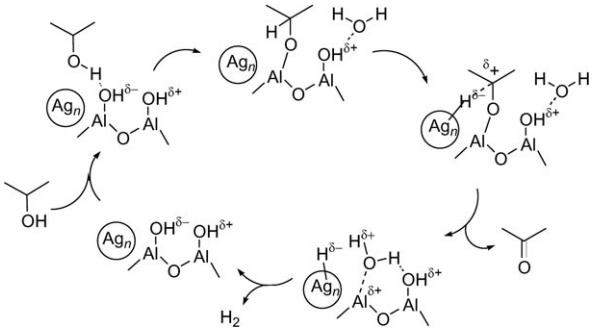

Scheme 1. Proposed mechanism for the alcohol dehydrogenation by Ag/Al_2O_3.

If the surface of alumina is highly dehydrated, the above catalytic cycle can be written as follows [Eq. (5)–(7)], where Al_{CUS} and $Al–O^{\delta-}$ represent the surface Lewis acid and Lewis base sites, respectively.:

$$(CH_3)_2CHOH + Al_{CUS} + Al–O^{\delta-} \rightarrow (CH_3)_2CH–O–Al + Al–OH^{\delta+} \quad (5)$$

$$R_2CH–O–Al + Ag_n \rightarrow (CH_3)_2C{=}O + Al_{CUS} + Ag_n–H^{\delta-} \quad (6)$$

$$Ag_n–H^{\delta-} + Al–OH^{\delta+} \rightarrow H_2 + Al–O^{\delta-} + Ag_n \quad (7)$$

Although this tentative mechanism may not be operative under the conditions of the catalytic experiments in this study, under which the catalyst cannot be highly dehydrated, the mechanism also indicates the importance of cooperation of acid–base sites with silver sites. The base sites are needed for proton abstraction from alcohol, the silver site is indispensable in C–H dissociation step, and the acid sites promote the release of dihydrogen.

Origin of size- and support-specific silver catalysis: In this section we discuss mechanistic reasons for the strong effects of the particle size and oxidation state of the silver species (Figures 2, 3) and the oxide support (Figure 4) on the basis of the in situ FTIR result (Figures 5, 6). To check the ability of ionic Ag^+ species on alumina to activate the α-C–H bond of 2-propoxide, we performed in situ IR experiments with Ag/Al_2O_3-0.5 under the same conditions as in Figure 6. Note that most of the silver species in Ag/Al_2O_3-0.5 are present as Ag^+ ions dispersed on the alumina surface (Figure 1). It was found that 2-propoxide species on this catalyst did not convert to acetone at 373 K (result not shown). This indicates that the silver cluster is necessary in the α-C–H activation step. It is well known that the numbers of corners, edges, and flat surfaces on metal nanoparticles change with particle size. Statistic calculations for Au, which possesses a similar atomic diameter (0.288 nm) to Ag (0.289 nm), were reported by Janssens et al.,[2] who assumed Au clusters shaped as the top half of a truncated octahedron. It has been shown that that the fraction of Au corner atoms decreases from ca. 64% to ca. 16% when the average size increases from 0.8 nm to 1.6 nm, whereas the fractions of edge and plane Au atoms increase slightly. Thus, below 2 nm, the fractions of Ag atoms at corner sites decease dramatically with Ag particle size. A sharp drop in TOF per surface Ag atom in a size below 2 nm as shown in Figure 3 suggests that the alcohol dehydrogenation by Ag/Al_2O_3 catalyst is a structure-sensitive reaction and that the corner Ag atoms might be the active species. In view of the role of the silver cluster proposed in the above section, it is suggested that corner Ag atoms play an important role in the α-C–H activation step.

With regard to the support effect, the result shown in Figure 4 demonstrates that both supports with low electronegativity (basic oxides) and oxides with high electronegativity (an acidic oxide, SiO_2) gave low yields, whereas the support with a moderate acid and basic nature—alumina—gave the highest yield. As mentioned above, the spectrum for propan-2-ol adsorption on MgO is basically identical to that for Al_2O_3 (Figure 5), indicating the formation of 2-propoxide groups on the surface of both these oxides. When propan-2-ol was introduced onto SiO_2, on the other hand, the bands due to 2-propoxide groups were hardly observed (Figure 5).

The chemisorption and reaction of propan-2-ol on some metal oxides have been extensively studied.[49,50,56,57] It is established that the initial step of the dissociative adsorption of alcohols on metal oxides is proton abstraction by a surface basic site. The surface of silica does not have such sites and hence cannot form 2-propoxide groups. The low catalytic activity of Ag/SiO_2 for alcohol dehydration can therefore be explained as follows: the basicity of the surface OH groups on silica is too weak to abstract proton from alcohol.

IR spectra for propan-2-ol adsorption on Ag/MgO-5 are shown in Figure 6B. The spectrum taken immediately after propan-2-ol adsorption ($t=60$ s) showed bands due to 2-propoxide groups, and the spectral feature is basically identical to those for Ag/Al_2O_3-5 and MgO (Figure 5). There are two remarkable differences between the spectra of Ag/Al_2O_3-5 and Ag/MgO-5. The band around 1640 cm^{-1} due to the HOH bending vibration of adsorbed water was not observed in the case of Ag/MgO-5. In the OH stretching region the band around 3300 cm^{-1} due to hydrogen-bonded water is negligible, whereas a band at 3627 cm^{-1} is observed. The band at 3627 cm^{-1} has been assigned to a hydrogen-bonded Mg–OH···O species, where O represents an adjacent surface oxygen atom.[58] At $t=300$ s, a band due to adsorbed acetone was observed at 1700 cm^{-1}. The band due to Mg–OH was shifted slightly to 3560 cm^{-1} but remained after 1200 s. In contrast, the hydrogen-bonded water on Ag/Al_2O_3 was practically absent after 1200 s. From these results, it is suggested that silver clusters on Ag/MgO-5 catalyze hydride elimination from the 2-propoxide group on MgO to produce acetone and water, which may react with a coordinatively unsaturated Mg site to produce Mg–OH. The protonic (electrophilic) nature of the surface OH groups for MgO is weaker than that in alumina, and so Mg–OH groups are less reactive with nucleophilic hydride species on silver clusters to produce hydrogen molecules. When the oxidation of 4-methylbenzyl alcohol was performed under oxygen as the hydrogen accepter, silver clusters on the support with low electronegativity (basic character) showed higher activity than under oxygen-free conditions (Figure 4). This supports the idea that under the oxygen-free conditions protonic (electrophilic) OH groups play an important role in the removal of hydride species from the silver sites. The acid-assisted decomposition of silver hydride is supported by the experimental evidence of a similar system reported by Baba et al.[14–16] By in situ ^1H MAS NMR, they studied the thermal stability of silver hydride species in zeolite, a porous aluminosilicate with Brønsted acid sites, and made the direct observation that hydride species on Ag clusters reacted with acidic protons to form H_2 and Ag_3^+ clusters at 353 K.[14–16]

From the above discussions, the volcano-shaped correlation between the electronegativity and alcohol dehydration activity (Figure 4) can be explained as follows. The basic (nucleophilic) OH groups present on the oxide surface are responsible for the formation of alkoxide intermediates, but their strongly basic natures will reduce the protonic nature of water (or M–OH species). As a consequence, the rate of alcohol dehydrogenation is reduced by slow removal of hydride species. On the other hand, with acidic or neutral metal oxide (SiO_2), dissociative adsorption of propan-2-ol is diminished by the weak nucleophilic character of the surface OH groups.

Conclusion

The alumina-supported silver cluster catalyst Ag/Al_2O_3 acts as an effective heterogeneous catalyst for oxidant-free alcohol dehydrogenation. The activity of the Ag/Al_2O_3 depends strongly on the charge and the size of silver species. Silver clusters, possibly having a slightly cationic natures, show higher rates per surface Ag site than monomeric Ag^+ ions and bulk Ag particle. Silver clusters with smaller particle sizes, especially below 1 nm, give higher intrinsic activity, indicating that this reaction is a structure-sensitive reaction demanding coordinatively unsaturated Ag sites, such as corner sites. It is proposed that the catalytic reaction proceeds in the following sequence: 1) reaction between the alcohol and a basic alumina OH group to yield the alkoxide and a water molecule adsorbed on alumina, 2) C–H activation of the alkoxide species by the silver cluster to form a silver hydride species and a carbonyl compound as the rate-determining step, and 3) H_2 desorption promoted by an alumina acid site. The proposed mechanism provides fundamental reasons for the higher activities of silver clusters on an acid–base bifunctional support (Al_2O_3) than on basic (MgO and CeO_2) or acidic to neutral (SiO_2) ones. Cooperative basic sites at the silver–support interface facilitate binding of the alcohol substrate to give the alkoxide intermediate on alumina. Protonic (electrophilic) OH groups at the interface facilitate the removal of hydride species from the silver sites to regenerate coordinatively unsaturated sites on the silver clusters.

Silver is less expensive than PGM elements, but it has been regarded as less reactive in C–H activation catalysis. Fundamental information in this study, demonstrating design of new alcohol dehydrogenation catalysts by use of a combination of size-controlled silver and acid–base bifunctional inorganic ligands, should accelerate research in the area of C–H activation catalysis and allows chemists to design practical PGM-free catalysts without using organic ligands.

Experimental Section

General: The GC (Shimadzu GC-17 A) and GCMS (Shimadzu GC-17 A) analyses were carried out with an Rtx-65 capillary column (Shimadzu) and nitrogen as the carrier gas. Commercially available organic and inorganic compounds were used without further purification. [D_2]propan-2-ol (98 atom% D) was purchased from Aldrich. The commercially available PGM-based heterogeneous catalysts Ru/C (Ru = 5 wt%, AC4504), Ru/Al_2O_3 (Ru = 5 wt%, AA-4501), Pd/C (Pd = 5 wt%, AC-2501), and Pd/Al_2O_3 (Pd = 5 wt%, AA-2501) were purchased from N.E. Chemcat Corporation.

Catalyst preparation: Ag/Al_2O_3 catalysts were prepared by impregnating γ-AlOOH (Catapal B alumina purchased from Sasol) with an aqueous solution of silver nitrate, followed by evaporation to dryness at 393 K. Before each catalytic or spectroscopic experiment, the precursor was calcined in air at 873 K for 1 h. The Ag/Al_2O_3 catalysts are designated as Ag/Al_2O_3-x, where x is the silver loading (wt%). Ag/Al_2O_3-5 was used as a standard catalyst. CeO_2 (JRC-CEO-1) and MgO (JRC-MGO-1) were supplied by the Catalysis Society of Japan. SiO_2 (Q-15) was supplied by Fuji Silysia Chemical. ZrO_2 was prepared by hydrolysis of zirconium oxynitrate 2-hydrate in distilled water by gradual addition of an aqueous NH_4OH solution (1.0 mol dm^{-3}), filtration of precipitate, washing three times with distilled water, and drying at 373 K for 24 h in air. Ag/MO_x catalysts (Ag = 5 wt%, MO_x = CeO_2, MgO, ZrO_2, SiO_2) were prepared by impregnation of an oxide support with an aqueous solution of silver nitrate, followed by evaporation to dryness at 393 K and by calcination in air at 773 K for 3 h.

In situ FTIR: In situ IR spectra were recorded with a JASCO FT/IR-620 instrument fitted with a quartz IR cell with CaF_2 windows and connected to a conventional flow reaction system. The sample was pressed into a self-supporting wafer (50 mg) and mounted in the quartz IR cell. Spectra were measured with accumulation of 20 scans at a resolution of 4 cm^{-1}. A reference spectrum of the catalyst wafer in He taken at the measurement temperature was subtracted from each spectrum. Prior to each experiment the catalyst disk was heated in an O_2/He (10%) flow (100 cm^3 min^{-1}) at 823 K for 1 h, followed by cooling to the desired temperature and purging for 30 min in He.

XAFS: Ag K-edge Quick XAFS measurements were performed in transmission mode at the BL01B1 in the SPring-8. The storage ring was operated at 8 GeV. A Si(111) single crystal was used to obtain a monochromatic X-ray beam. For Ag/Al_2O_3 samples, a self-supported wafer form of the sample (0.1–1.0 g) of ca. 10 mm diameter was placed in a quartz in situ cell[59] in an O_2 flow (10%) diluted with He (200 cm^3 min^{-1}) at atmospheric pressure. For Ag/MO_x catalysts (MO_x = CeO_2, MgO, ZrO_2, SiO_2), samples pre-reduced for 10 min under H_2 (1 atm) at 373 K were sealed in cells made of polyethylene under ambient atmosphere, and XAFS spectra were taken at room temperature. Analysis of the extended X-ray absorption fine structure (EXAFS) was performed with the aid of the REX version 2.5 program (RIGAKU). The Fourier transformation of the k^3-weighted EXAFS oscillation from k-space to r-space was performed over the 30–140 nm^{-1} range to obtain a radial distribution function. The inversely Fourier filtered data were analyzed with a conventional curve fitting method in the k range of 48–140 nm^{-1}. For the curve-fitting analysis of Ag/Al_2O_3 samples, the empirical phase shift and amplitude functions for Ag–Ag and Ag–O shells were extracted from the data for Ag foil and Ag_2O, respectively, measured at 573 K. For the curve-fitting analysis of Ag/MO_x samples, the empirically determined phase shift and amplitude functions for Ag–Ag and Ag–O shells were extracted from the data for Ag foil and Ag_2O, respectively, measured at room temperature.

Typical procedures for the dehydrogenation of alcohols: Before a reaction, Ag/Al_2O_3 or Ag/MO_x (MO_x = CeO_2, MgO, ZrO_2, SiO_2) was treated in the reaction vessel for 10 min under H_2 (1 atm) at 573 or 373 K, respectively, allowed to cool to room temperature, and then exposed to the ambient atmosphere. Note that XANES and EXAFS results (not shown) showed that the silver species in Ag/MO_x were nearly completely reduced. The prereduced Ag/Al_2O_3-5 (0.05 g, 2.0 mol% Ag) was added to the mixture of toluene (3.0 mL) and benzyl alcohol (0.11 g, 1 mmol) in a reaction vessel fitted with a condenser, and the system was placed under N_2. The resulting mixture was vigorously stirred at 373 K. The reaction mixtures were analyzed by GC and GCMS. Levels of conversion of alcohols and yields of carbonyl compounds were determined by GC with n-dodecane as an internal standard. The amounts of evolved H_2 was determined by gas chromatography with a thermal conductivity detector (TCD), molecular sieve (5 Å) column, and Ar carrier.

[1] M. Haruta, N. Yamada, T. Kobayashi, S. Iijima, *J. Catal.* **1989**, *115*, 301.
[2] T. V. W. Janssens, B. S. Clausen, B. Hvolbak, H. Falsig, C. H. Christensen, T. Bligaard, J. K. Norskov, *Top. Catal.* **2007**, *44*, 15.
[3] T. Ishida, M. Nagaoka, T. Akita, M. Haruta, *Chem. Eur. J.* **2008**, *14*, 8456.
[4] H. Tsunoyama, H. Sakurai, Y. Negishi, T. Tsukuda, *J. Am. Chem. Soc.* **2005**, *127*, 9374.
[5] H. Miyamura, R. Matsubara, Y. Miyazaki, S. Kobayashi, *Angew. Chem.* **2007**, *119*, 4229; *Angew. Chem. Int. Ed.* **2007**, *46*, 4151.
[6] A. Abad, A. Corma, H. Garcia, *Chem. Eur. J.* **2008**, *14*, 212.

[7] F.-Z. Su, J. Ni, H. Sun, Y. Cao, H.-Y. He, K.-N. Fan, *Chem. Eur. J.* **2008**, *14*, 7131.
[8] G. J. Hutchings, *Catal. Today* **2007**, *122*, 196.
[9] T. Sun, K. Seff, *Chem. Rev.* **1994**, *94*, 857.
[10] A. Henglein, *Chem. Rev.* **1989**, *89*, 1861.
[11] G. A. Ozin, M. D. Baker, J. Godber, *J. Phys. Chem.* **1984**, *88*, 643.
[12] H. Beyer, P. A. Jacobs, J. B. Uytterhoeven, **1977**, *73*, 1111.
[13] Y. Suzuki, N. Matsumoto, T. Ainai, T. Miyanaga, H. Hoshino, *Polyhedron* **2005**, *24*, 685.
[14] T. Baba, Y. Tohjo, T. Takahashi, H. Sawada, *Catal. Today* **2001**, *66*, 81.
[15] T. Baba, H. Sawada, T. Takahashi, M. Abe, *Appl. Catal. A* **2002**, *231*, 55.
[16] T. Baba, Y. Iwase, K. Inazu, D. Masih, A. Matsumoto, *Microporous Mesoporous Mater.* **2007**, *101*, 142.
[17] P. Claus, H. Hofmeister, *J. Phys. Chem. B* **1999**, *103*, 2766.
[18] Y. Chen, C. Wang, H. Liu, J. Qiu, X. Bao, *Chem. Commun.* **2005**, 5298.
[19] Z. Qu, W. Huang, M. Cheng, X. Bao, *J. Phys. Chem. B* **2005**, *109*, 1584.
[20] K. Shimizu, A. Satsuma, *Phys. Chem. Chem. Phys.* **2006**, *8*, 2677.
[21] K. Shimizu, M. Tsuzuki, K. Kato, S. Yokota, K. Okumura, A. Satsuma, *J. Phys. Chem. C* **2007**, *111*, 950.
[22] K. Shimizu, K. Sugino, K. Kato, S. Yokota, K. Okumura, A. Satsuma, *J. Phys. Chem. C* **2007**, *111*, 1683.
[23] T. Mitsudome, Y. Mikami, H. Funai, T. Mizugaki, K. Jitsukawa, K. Kaneda, *Angew. Chem.* **2008**, *120*, 144; *Angew. Chem. Int. Ed.* **2008**, *47*, 138.
[24] T. Mitsudome, S. Arita, H. Mori, T. Mizugaki, K. Jitsukawa, K. Kaneda, *Angew. Chem.* **2008**, *120*, 8056; *Angew. Chem. Int. Ed.* **2008**, *47*, 7938.
[25] T. Matsumoto, M. Ueno, N. Wang, S. Kobayashi, *Chem. Asian J.* **2008**, *3*, 196.
[26] K. Mori, T. Hara, T. Mizugaki, K. Ebitani, K. Kaneda, *J. Am. Chem. Soc.* **2004**, *126*, 10657.
[27] K. Yamaguchi, N. Mizuno, *Chem. Eur. J.* **2003**, *9*, 4353.
[28] M. S. Sigman, D. R. Jensen, *Acc. Chem. Res.* **2006**, *39*, 221.
[29] T. Mallat, A. Baiker, *Chem. Rev.* **2004**, *104*, 3037.
[30] F. Zaccheria, N. Ravasio, R. Psaro, A. Fusi, *Chem. Eur. J.* **2006**, *12*, 6426.
[31] G. R. A. Adair, J. M. J. Williams, *Tetrahedron Lett.* **2005**, *46*, 8233.
[32] G. B. W. L. Ligthart, R. H. Meijer, M. P. J. Donners, J. Meuldijk, J. A. J. M. Vekemans, L. A. Hulshof, *Tetrahedron Lett.* **2003**, *44*, 1507.
[33] J. H. Choi, N. Kim, Y. J. Shin, J. H. Park, J. Park, *Tetrahedron Lett.* **2004**, *45*, 4607.
[34] H. Junge, M. Beller, *Tetrahedron Lett.* **2005**, *46*, 1031.
[35] J. Zhang, M. Gandelman, L. J. W. Shimon, H. Rozenberg, D. Milstein, *Organometallics* **2004**, *23*, 4026.
[36] K.-I. Fujita, N. Tanino, R. Yamaguchi, *Org. Lett.* **2007**, *9*, 109.
[37] Y. Ando, M. Yamashita, Y. Saito, *Bull. Chem. Soc. Jpn.* **2003**, *76*, 2045.
[38] M. Yamashita, T. Kawamura, M. Suzuki, Y. Saito, *Bull. Chem. Soc. Jpn.* **1991**, *64*, 272.
[39] W.-H. Kim, I. S. Park, J. Park, *Org. Lett.* **2006**, *8*, 2543.
[40] T. Mitsudome, Y. Mikami, K. Ebata, T. Mizugaki, K. Jitsukawa, K. Kaneda, *Chem. Commun.* **2008**, 4804.
[41] R. Noyori, T. Ohkuma, *Angew. Chem.* **2001**, *113*, 40; *Angew. Chem. Int. Ed.* **2001**, *40*, 40.
[42] H. Grützmacher, *Angew. Chem.* **2008**, *120*, 1838; *Angew. Chem. Int. Ed.* **2008**, *47*, 1814.
[43] S. E. Clapham, A. Hadzovic, R. H. Morris, *Coord. Chem. Rev.* **2004**, *248*, 2201.
[44] M. Ito, A. Osaku, A. Shiibashi, T. Ikariya, *Org. Lett.* **2007**, *9*, 1821.
[45] A. Jentys, *Phys. Chem. Chem. Phys.* **1999**, *1*, 4059.
[46] C. Morterra, G. Magnacca, *Catal. Today* **1996**, *27*, 497.
[47] M. Digne, P. Sautet, P. Raybaud, P. Euzen, H. Toulhoat, *J. Catal.* **2004**, *226*, 54.
[48] G. Busca, *Phys. Chem. Chem. Phys.* **1999**, *1*, 723.
[49] P. F. Rossi, G. Busca, V. Lorenzelli, O. Saur, J. C. Lavalley, *Langmuir* **1987**, *3*, 52.
[50] M. I. Zaki, M. A. Hasan, L. Pasupulety, *Langmuir* **2001**, *17*, 4025.
[51] A. R. McInroy, D. T. Lundie, J. M. Winfield, C. C. Dudman, P. Jones, D. Lennon, *Langmuir* **2005**, *21*, 11092.
[52] H. A. Al-Abadleh, V. H. Grassian, *Langmuir* **2003**, *19*, 341.
[53] A. R. McInroy, D. T. Lundie, J. M. Winfield, C. C. Dudman, P. Jones, S. F. Parker, D. Lennon, *Catal. Today* **2006**, *114*, 403.
[54] A. Dyan, P. Cenedese, P. Dubot, *J. Phys. Chem. B* **2006**, *110*, 10041.
[55] M. I. Zaki, M. A. Hasan, F. A. Al-Sagheer, L. Pasupulety, *Langmuir* **2000**, *16*, 430.
[56] D. Kulkarni, I. E. Wachs, *Appl. Catal. A* **2002**, *237*, 121.
[57] M. Seman, M J. N. Kondo, K. Domen, C. Reed, S. T. Oyama, *J. Phys. Chem. B* **2004**, *108*, 3231.
[58] C. Chizallet, G. Costentin, M. Che, F. Delbecq, P. Sautet, *J. Am. Chem. Soc.* **2007**, *129*, 6442.
[59] K. Okumura, K. Yoshino, K. Kato, M. Niwa, *J. Phys. Chem. B* **2005**, *109*, 12380.

Received: October 27, 2008
Published online: January 21, 2009

